2011 IEEE/RSJ International Conference on
Intelligent Robots and Systems
September 25-30, 2011. San Francisco, CA, USA

Varying spring preloads to select grasp strategies in an adaptive hand

Daniel Aukes*, Barrett Heyneman*, Vincent Duchaine† and Mark R. Cutkosky*

***Abstract*— We describe an underactuated hand mechanism that is able to adopt a wide range of grasp types by varying the internal forces in its fingers. The adjustment is accomplished by varying the preloads of springs, which affect the grasp stability and stiffness for large and small objects. Preload adjustment can be accomplished with low power, non-backdrivable actuators in the fingers. The analysis is presented first for a planar, two-fingered hand to illustrate the trends and tradeoffs associated with variations in preload. The results are then applied numerically to a three fingered hand with three phalanges per finger. This design is a prototype for a hand to be used in an underwater oil drilling platform under conditions of low friction and uncertain object locations.**

***Index Terms*— underactuation, robotic hand, parallel linkage, kinematic design,**

I. Introduction

Many underactuated hands for robotics and prosthetics have been developed over the last 30 years. They aim to strike a balance between versatility and complexity, grasping a wide range of shapes and sizes while minimizing the number of actuators, simplifying control, and reducing the dependence on sensing [1], [2], [3], [4], [5], [6]. In these hands, springs or compliant elements are often used to provide passive control over the order in which phalanges close upon an object. The compromises associated with underactuation and the kinematics required to perform stable wrap grasps, however, generally limit the repertoire of available grasps.

To expand their versatility, some underactuated hands are able to wrap around small objects with just a few phalanges [1], however this typically requires running the fingers into each other and is relatively uncontrolled. Other hands [2], [7] are designed to keep their fingertips parallel if the proximal phalanges do not contact an object, allowing a single underactuated hand to achieve both wrap grasps for medium and large objects and pinch grasps for small or thin objects. The pinch grasps, however, require accurate object placement to ensure proper contact location, and rely on friction to stabilize the object. In general, grasp type selection prior to initial contact is unavailable in highly-underactuated hands.

We present the design of an adaptive hand that has one primary actuator per finger and secondary actuators in the remaining joints that control the preloading of internal springs.

The authors are with: *the Department of Mechanical Engineering, Stanford University, Stanford, CA, United-States. †École de Technologie Supérieure, Montréal, Québec, Canada. danaukes@stanford.edu, heyneman@stanford.edu, vincent.duchaine@etsmtl.ca, cutkosky@stanford.edu.

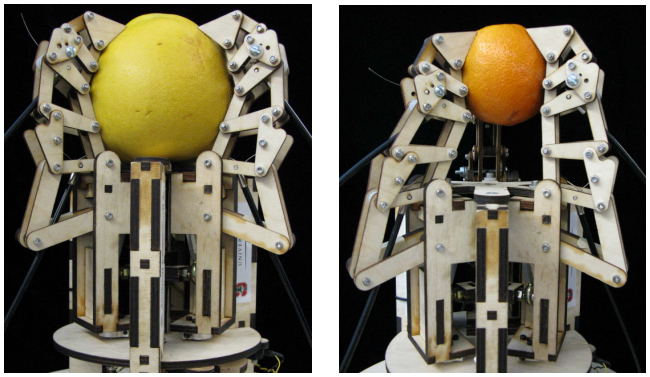

(a) (b)

Fig. 1: The Seabed Rig hand in two configurations: (a) grasping a grapefruit with a spherical wrap grasp, and (b) grasping an orange with a spherical "power-pinch" grasp

The hand shown in Fig. 1 is an early prototype for the hand of a large underwater robot to be used in an automated oil drilling rig [8]. As the only robotic hand available within the fully automated rig, it will be required to securely grasp both large and small objects from a minimum diameter of 40 mm to a maximum of 400 mm in a slippery, muddy environment. The initial prototype is a 1/4 scale model, which translates to grasping objects with diameters ranging from 10 mm to 100 mm (i.e., to 3/4 of the length of a finger) without relying on friction.

Demers *et al.* [9] showed that adding a second actuator to a highly underactuated hand increases the range of stable grasps. In addition, Ciocarlie *et al.* [10] show the effect that changing joint stiffness can have on the range of graspable objects, but use the analysis as a design tool for a fixed stiffness. Here, we distinguish our design with the following points. First, the mechanism used to control the internal spring preloading is a low-power, non-backdriveable motor and lead-screw which add only moderate cost and complexity to the system. Instead of actively controlling forces in the hand it is responsible for altering the passive adaptability of the hand, putting much less demand on power and speed. In this sense, it allows one to change between different compliance approaches in a manner similar to that discussed in [11].

By changing the balance of forces in the finger, different hand postures become available for grasping objects than would work with a traditional wrap grasp. One such posture, which we refer to as a "power pinch" (Figs. 1b and 2c),

978-1-61284-456-5/11/$26.00 ©2011 IEEE

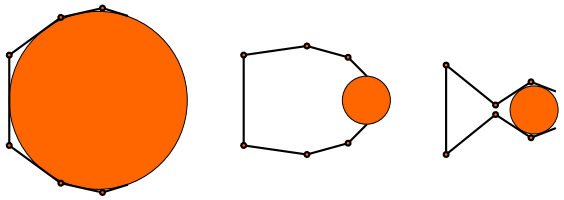

Fig. 2: Three grasp types: (a)underactuated wrap, (b)fingertip-only pinch, and (c)"power pinch"

holds small objects securely between the second and third phalanx, a particularly useful strategy under conditions of low friction and uncertain object loads and locations. This particular grasp is an important design feature for the Seabed Rig hand, allowing it to grasp small objects with as many contacts as possbile when wrap grasps are too large for the object.

In the following sections we present the analysis of the secondary actuation system first in a simplified fingertip model. We show how varying spring preloads in such a finger increases the range of graspable objects and gives us the ability to adapt our grasp for different conditions. We then analyze the three-finger Seabed Rig hand with a quasi-static simulation that shows the advantage of variable spring preloads in a three-phalanx finger. Finally, we discuss the implications of building such a device, potential use cases, and directions for future work.

II. Spring Loading Mechanism Concept

A spring loading mechanism is shown in Fig. 3, consisting of a compression spring placed in series with an adjustable screw, between two opposite points in a four-bar linkage. A small motor rotates the screw, advancing or retracting a nut. When the finger is unconstrained (e.g., before grasping) this adjustment changes the equilibrium configuration of the linkage, according to the free length of the spring plus the screw length. If the finger is contacting an object, and the configuration is fixed, this adjustment changes the internal force, equivalent to preloading a spring.

Due to the nature of the four-bar mechanism, even a linear spring will produce a substantially nonlinear endpoint stiffness. The parameters of the linkage also affect the force distribution and closing properties of the hand, and have been studied extensively [12], [7], including the effects of compliance [13]. However, while the connection points of the spring affect its nonlinearity with respect to changes in configuration, they do not affect the finger kinematics or transmission ratios.

In the following analysis we do not claim an optimal solution but show that one can independently vary finger kinematics and spring characteristics for specific, desirable grasping properties.

III. Fingertip Analysis

Before considering the Seabed Rig hand, with three fingers each having two spring-loading mechanisms and three phalanges, we consider a simple, planar hand with two phalanges and a single spring. The analysis for this example is relatively straightforward and illustrates the trade-offs possible with different values of spring stiffness and preloading. The conclusions from this section motivate the numerical simulations of the Seabed Rig hand in the subsequent section.

Understanding the effect of the proposed mechanism in our hand requires selecting metrics that work well when evaluating adaptive or underactuated hands, since form or force-closure metrics generally apply to fully actuated hands. Kragten *et al.* [14] review many metrics used for underactuated hands, focusing in particular on *i)* a hand's ability to achieve equilibrium when grasping, and *ii)* a hand's ability to maintain a grasp in the presence of disturbance forces. Balasubramanian *et al.* [11] have also studied hand configuration changes with regard to external disturbances; however their analysis is based on the assumption of a highly underactuated hand and does not consider configuration changes due to changes in internal forces.

We consider a system in which two opposed, two-phalanges planar fingers, symmetrically grasp a circle (Fig. 3). We assume all contacts in this analysis are frictionless point contacts, which reduces the wrench space between the finger and the grasped object to normal forces only, keeping the analysis tractable and allowing us to draw meaning from potential energy curves as in Fig. 6b. If we assume grasping constraints that enforce contact on each phalanx, the dimension of the wrench between the finger and the grasped object is the same as the dimension of the wrench between the finger and the motor/spring combination. These assumptions about object shape, contact, and friction make it possible to calculate grasping forces as a function of our motor torque and spring force, but are also realistic in the context of a muddy, slippery environment with many

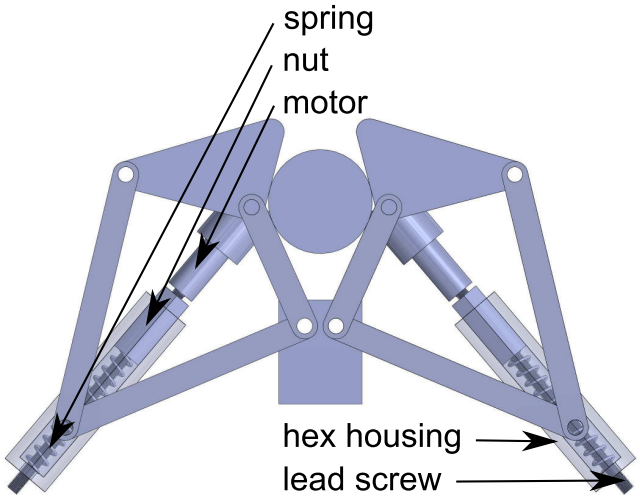

Fig. 3: The spring adjustment mechanism

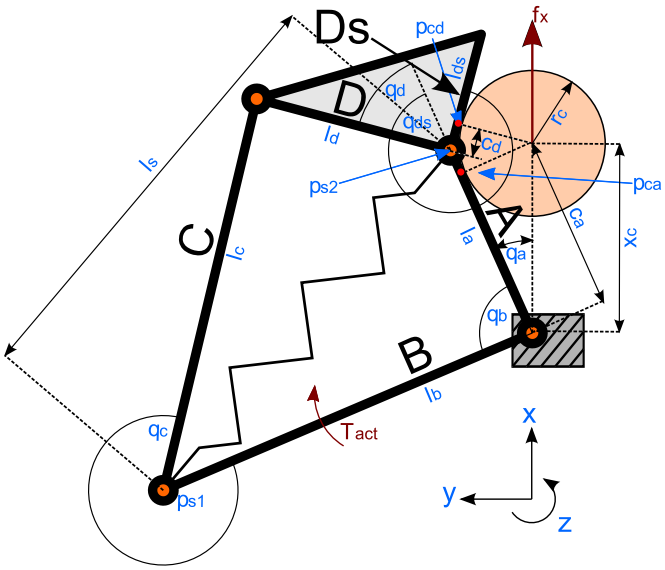

Fig. 4: Description of variables used in analytic model

compact and cylindrical objects.

A. Analytical Model

Expanded details of the following derivation can be found in Appendix A. The finger has two degrees of freedom, from which all the joint angles of the linkage can be determined. Using the notation of McCarthy [15], we write the closed-loop kinematic equations and express the matrix $\mathbf{C}$, which relates dependent configuration variables to independent variables as in [16]. For our model we define those variables as

$$\mathbf{q}_{ind} = \begin{bmatrix} q_a \\ q_d \end{bmatrix}, \mathbf{q}_{dep} = \begin{bmatrix} q_b \\ q_c \end{bmatrix}, \tag{1}$$

such that

$$\dot{\mathbf{q}}_{dep} = \mathbf{C}\dot{\mathbf{q}}_{ind}. \tag{2}$$

Our finger's main actuator is placed on the input side of the four bar linkage, at link B. We then define $\mathbf{J}_{act}$, the 1×2 Jacobian matrix relating the actuator angle, $\mathbf{q}_{act}$, to $\mathbf{q}_{ind}$, and $\mathbf{J}_s$, the 1×2 Jacobian matrix relating the length of the spring, $\mathbf{l}_s$, to $\mathbf{q}_{ind}$, such that:

$$\dot{q}_{act} = \mathbf{J}_{act}\dot{\mathbf{q}}_{ind} \tag{3}$$

$$\dot{l}_s = \mathbf{J}_s\dot{\mathbf{q}}_{ind} \tag{4}$$

The spring Jacobian deriviation is similar to that found in [13], but instead provides for placing linear springs between two points in the four bar linkage instead of torsional springs in the joint.

Finally, we define the 4×2 matrix $\mathbf{J}_c$ as the Jacobian relating the motion of the contact points, $\mathbf{p}_{ca}$ and $\mathbf{p}_{cd}$, to $\mathbf{q}_{ind}$. Because we are only considering normal forces at those contacts, we reformulate the Jacobian through a 2×4 force selection matrix, $\mathbf{F}_{norm}$, to remove tangential components, after which we have

$$\begin{bmatrix} \dot{\mathbf{p}}_{ca} \\ \dot{\mathbf{p}}_{cd} \end{bmatrix} = \mathbf{J}_c\dot{\mathbf{q}}_{ind} \tag{5}$$

$$\mathbf{J}_{cn} = \mathbf{F}_{norm}\mathbf{J}_c \tag{6}$$

Equipped with the required Jacobians, we can use virtual work to derive the conditions for static equilibrium,

$$\left(\mathbf{J}_{act}^T\tau_{act} + \mathbf{J}_{cn}^T\mathbf{f}_{cn} - \mathbf{J}_s^T f_s\right)\dot{\mathbf{q}}_{ind} = 0, \tag{7}$$

where τ_{act} is the actuator torque and $\mathbf{f}_{cn}$ is the vector of normal contact forces on phalanx 1 and 2, respectively, and $f_s = -k_s\left(l_s - l_0\right)$, with l_0 defined as the spring preload. This allows us to solve for $\mathbf{f}_{cn}$,

$$\mathbf{f}_{cn} = -\mathbf{J}_{cn}^{-T}\mathbf{J}_{in}\mathbf{f}_{in}, \tag{8}$$

where

$$\mathbf{f}_{in} = \begin{bmatrix} \tau_{act} \\ f_s \end{bmatrix}, \mathbf{J}_{in} = \begin{bmatrix} \mathbf{J}_{act} \\ -\mathbf{J}_s \end{bmatrix}. \tag{9}$$

The final requirement for a full analytical model is generation of the contact constraints; namely that both phalanges are in contact with the circle. With those constraints, the configuration of the fingers is completely defined by the coordinate x_c of the circle's center along the x-axis. First, the position of the circle and the angle of link A are related by

$$q_a = \arcsin\left(\frac{r_c}{x_c}\right). \tag{10}$$

The two contact locations can be expressed as

$$c_a = x_c\cos(q_a) \quad \text{and} \quad c_d = l_a - c_a. \tag{11}$$

Finally, the angle of the contact surface of link D can be defined by

$$q_{ds} = 2\arctan\left(\frac{r_c}{c_d}\right) + \pi. \tag{12}$$

B. Stability

One can use the model in the previous section to investigate how the spring preload mechanism can increase stability and increase the range of graspable objects for a variety of preloads, object radii, and object positions. Fig. 4 and Table I detail the variables and their associated values used to generate these data. (8) is used to calculate the contact normal forces for a given object's size and position generated from (10) - (12), which are added and resolved into global x and y components. Forces along the y-axis are ignored, as the grasp is assumed to be symmetric.

When we consider the stability region for the two-phalanx model as a function of object size and disturbance force, the benefit of a variable-preload mechanism is apparent. Fig. 5 shows stable regions and demonstrates the effect that varying preload can have on objects of different size. Object size and

TABLE I: Parameters used for Fingertip Analysis

variable	*value*
q_{ds}	$q_d - \frac{\pi}{2}$
τ_{act}	.03N-mm
k_s	1N/mm
l_a	50mm
l_b	$2 * l_a$ = 100mm
l_c	$2 * l_a$ = 100mm
l_d	$1 * l_a$ = 50mm
l_{ds}	$0.6 * l_a$ = 30mm

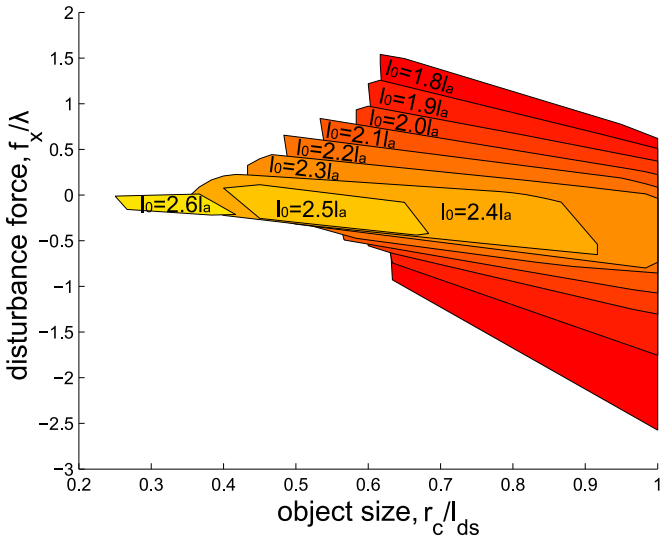

Fig. 5: Regions of graspable object size/external force combinations, for various preload values, l_0. Increasing the preload increases the object size range at the expense of disturbance force rejection when grasping larger objects.

external force have been scaled relative to the length of the distal phalanx, l_{ds}, and input torque divided by the length of the proximal phalanx, $\lambda = \tau_{act}/l_a$, respectively.

Smaller objects can be grasped as preload (l_0) increases, while the range of disturbance forces rejected without friction decreases. Larger objects can be grasped at lower preloads, but those objects can withstand much higher disturbance forces, f_x/λ. If a preload were to be chosen at design-time the hand would operate in only one of these regions, while a variable-preload mechanism allows the hand to operate in a region defined by their union. By using Fig. 5 to set our preload to an expected object size we are able to grasp a wider range of objects without having to sacrifice average grasp stability over that range.

Variable preload has utility not only for increasing the range of graspable objects, but for customizing grasps for different tasks. Once we know the size of the object we are grasping, we can vary preloads to suit the precision and force requirements of the task. Fig. 6a plots the external force required to hold a circle of radius $0.4l_a$ (where l_a is the length of the proximal phalanx, for scaling purposes) in static equilibrium at a given location along the x-axis, with each curve representing a different spring preload. The stable region of each curve is denoted by a solid line, corresponding to regimes in which contact forces are positive or zero [7]. The boundaries of these stable regions indicate the minimum and maximum external forces that each grasp can resist. Fig. 6b represents the change in energy required to move a stably grasped circle along the x-axis over the same range of spring preloads. The boundaries of these curves correspond to the same stable regions, the boundary values representing the maximum impact energy a grasp can sustain along the x-axis while remaining stable.

The slopes of the curves at $f_x = 0$ in Fig. 6a also indicate the effective interface stiffness between the object and the hand. At its highest preload, the effective spring stiffness is roughly 3 times higher than at its lowest. These data demonstrate that the spring preload mechanism allows some grasp optimization for quantities such as maximum disturbance force rejection, effective stiffness, and grasp

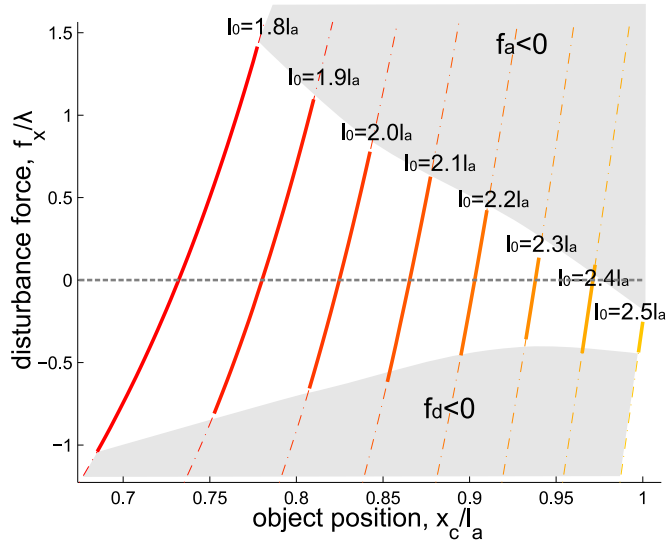

(a)

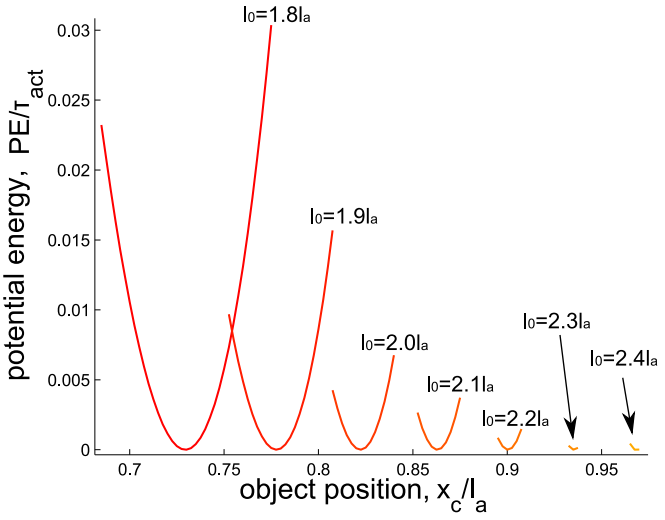

(b)

Fig. 6: (a) The x-component of forces (scaled by λ) required to hold the object along the x axis for a range of spring preloads. Solid lines indicate regions where both phalanges' normal forces are positive, their boundaries show the maximum force in either direction before the grasp fails. Shallower slopes for low preloads indicate low effective stiffness in the x-direction. (b) The relative potential energy (scaled by actuator torque) required to pull a cylindrical object from equilibrium over the range of preloads.

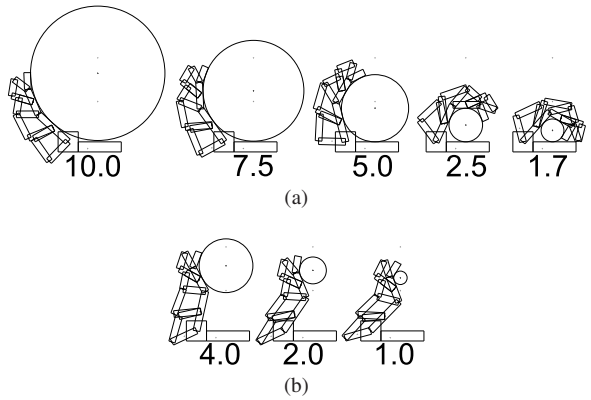

Fig. 7: Grasping range of the Seabed Rig Hand. With the ability to change spring preloads, the wrap grasp (a) is capable of grasping larger objects with a size range of 2:10, and the "power-pinch" grasp (b) is capable of grasping smaller objects in a size range of 1:4

posture (closer or farther from the palm).

IV. Seabed Rig Analysis

The Seabed Rig hand is designed to naturally wrap around objects with a series of two compact, double-stage four bar mechanisms. The spring adjustment mechanism is similar to but more complex than shown in Fig. 3. Cables in sleeves, attached to the finger links, transmit forces to the base of the hand, while torsional return springs provide a bias force for each degree of freedom. While this system exhibits similar grasping capabilities to the results of the following simulation, the cable system exhibits undesirable friction.

With two passive springs adjusted at the correct preload, the hand is able to wrap around a range of objects roughly between 20mm and 100mm, where 100mm corresponds to 3/4 the length of the fingers. With the same passive springs adjusted to new preloads, the same finger is able to grasp smaller objects, without friction, between only the second and third phalanx. This grasp, which we call a "power pinch," complements the range of graspable objects possible in the wrap by grasping objects between 10mm and 20mm. The range is small, but it expands the ratio of graspable objects from 1:5 to 1:10, a critical design component for our hand design, and the motivation for studying the effect of adding a variable-preload device.

A. Analysis

We have performed a quasi-static simulation in Working-Model2005 using kinematics of the SeabedRig Hand. Our analysis includes one variable-preload spring device in each of the two double-stage mechanisms. The spring preloads can be varied between two limits while the spring constants remain the same. A constant torque is applied to the input link of the base phalanx's transmission. Finally, a circular object is placed in the hand and a variable disturbance force is applied to the center of mass along the x-axis. The object is constrained to travel in the x-direction only, under the assumption that the grasp is held by three axisymmetric fingers. Friction and gravity are neglected in this analysis. A small amount of damping is added to the system to enable it to come to rest.

Just as in the two-phalanx analysis, the grasped object will come to rest at a specific location along the x-axis as a function of disturbance force and spring preload if it stays within its stable region. Small changes to the spring preloads and disturbance force result in incremental changes to the equilibrium location of the object. As in Fig. 6, The position/force curves in Fig. 8 give information regarding the stability of the grasp, the effective stiffness of the grasp, and the maximum disturbance forces that a particular set of preloads can resist for a given sized object.

Four cases were tested (Table II). As can be seen in Fig. 8, the hand is able to hold a 50mm object over a wide range of disturbance forces with a set of experimentally-optimized spring preloads (Case 1). Near the limit of its stability it adopts something close to a "power-pinch" configuration around $x_c = 80$mm. By using another set of preloads (Case 2), the hand is able to grasp a 20mm object in a "power-pinch" while rejecting a wide range of external disturbances around an equilibrium point. However, when the preload/object pairing is switched, performance drops, shown by the graphs of Case 3 and Case 4 in Fig. 8. Furthermore, the grasp in Case 3 is not even able to achieve equilibrium in the presence of zero external forces, as evidenced by the fact that the force profile does not cross zero. This simulation demonstrates that changing preloads can optimize frictionless or low-friction grasping performance over a particular size range and confirms that variable preload is necessary to grasp

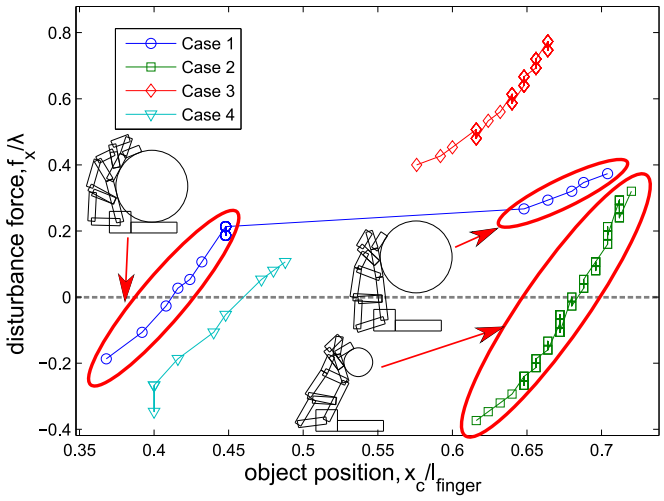

Fig. 8: A position-force plot is shown for four cases of the Seabed Rig hand. First, near-optimal spring preloads were found experimentally for each size object (Cases 1, 2). These cases are capable of rejecting a wide range of disturbance forces, and generally allow the object to travel within a wide range of positions before the grasp fails, as shown by the insets of the finger. In Cases 3, 4, those same preloads were used on the opposite object, with worse results.

TABLE II: Four test cases for Seabed Rig hand

Case	r_c	$l1_0$	$l2_0$
1	50mm	68mm	28mm
2	20mm	95mm	35mm
3	20mm	68mm	28mm
4	50mm	95mm	35mm

a wider range of objects than could be achieved with a fixed-length spring.

V. Discussion

Adding a spring-preload mechanism to an underactuated finger leads to increased grasp stability across a wider range of objects than a single preload can achieve. In a simple finger this mechanism changes the effective grasping forces but does not change the grasp. In more complicated fingers, the same underlying principle can be used to change the locations and contact conditions of the grasp, leading to gross changes in posture, advantageous for grasping an even larger range of objects.

Our analysis of the simple two-phalanx finger has also shown that there is not one *best* preload for any given object; by varying the preload one can trade/off between effective stiffness, maximum disturbance force/energy, and object posture relative to the hand. In real-world scenarios, such as the Seabed Rig underwater drilling platform, this trade-off can be quite important. The Seabed Hand is expected to pick up and move hoses or sections of drill pipe which get in the way of normal operation. While some of these objects are similar enough in size that a single preload would grasp both stably, the requirements of the two tasks may call for distinct properties. A piece of broken drill pipe, for example, is larger and more massive than a hose, and any accidental collisions between it and the environment will involve relatively more energy. For this reason a preload which maximizes the allowed disturbance energy may be the most appropriate. In contrast, the hose is more delicate and is likely attached at one or both ends, so a grasp that is incapable of applying large forces will better protect it. While the broken pipe may only need to be placed in a generally safe area, an errant hose may need to be tucked back into a specific routing configuration. This may require a stiffer interface for more precision, or that the hose be held farther from the palm so that it can be placed into a tighter space.

VI. Conclusion and Future Work

We have developed an adaptive robotic hand that is capable of changing its grasping style to accommodate both large and small objects. By changing the preload of internal springs we change the balance of internal forces, allowing the finger to adopt a range of poses beween a wrap and pinch grasp. We have presented an analytical model for calculating stability in a simple two-phalanx finger and verified it with the results from a numerical quasi-static simulation. We have also analyzed the Seabed Rig hand and shown that it can exhibit different grasp poses for different-sized objects. In addition, we have demonstrated that changing this spring preload is not only beneficial but necessary to optimize grasping performance for objects of different size under low-friction conditions.

While changing the preload in a hand can be beneficial, it comes at the cost of increased complexity due to additional motors. Several elements of this analysis lead us to conclude that the overall impact on complexity can be mitigated by appropriate component selection. The hand can adapt to a range of disturbance forces, eliminating the need for real-time force control. Actuators can therefore be small, low-power, non-backdriveable devices located within the finger. However, as with previous highly-underactuated hands [1], [2], [17], the resulting grasps are still adaptive. If a leadscrew-style transmission is used to change the spring preload, the spring itself protects the motor and transmission elements from shock and vibration. Substituting the proposed spring adjustment mechanism into the next-generation hand would reduce friction, weight, and complexity in a hand that may ultimately operate at the bottom of the ocean.

VII. Acknowledgements

This work was supported by Seabed Rig, AS. D. Aukes is supported by a SGF fellowship, and V. Duchaine by The Natural Sciences and Engineering Research Council of Canada (NSERC).

Appendix

A. Derivation of Two-Phalanx Analytical Model

The 2×2 matrix $\mathbf{C}$ is formed by considering the closed-loop kinematic equation of the four-bar mechanism,

$$\mathbf{0} = \begin{bmatrix} l_a + l_b \cos q_b - l_c \cos(q_b + q_c) + l_a \cos q_d \\ l_b \sin q_b - l_c \sin(q_b + q_c) + l_d \sin q_d \end{bmatrix}, \quad (13)$$

and taking the derivitave to find the relationship between independent and dependent velocity variables.

$$\mathbf{A}\dot{\mathbf{q}}_{ind} + \mathbf{B}\dot{\mathbf{q}}_{dep} = \mathbf{0}, \quad (14)$$

where $\mathbf{A}$ and $\mathbf{B}$ are the Jacobians of the loop equation with respect to $\mathbf{q}_{ind}$ and $\mathbf{q}_{dep}$. By solving for $\dot{\mathbf{q}}_{dep}$ we form $\mathbf{C}$ as

$$\mathbf{C} = -\mathbf{B}^{-1}\mathbf{A}. \quad (15)$$

The actuator, spring, and contact Jacobians ($\mathbf{J}_a$, $\mathbf{J}_s$, and $\mathbf{J}_c$, respectively) are all determined in a similar manner once we define the relevant variables and their relation to $\mathbf{q}_{ind}$ and $\mathbf{q}_{dep}$. Referring to Fig. 4 we see that

$$q_{act} = q_a + q_b \quad (16)$$

$$l_s = \|\mathbf{p}_{s1} - \mathbf{p}_{s2}\| \quad (17)$$

$$\mathbf{p}_{ca} = \begin{bmatrix} c_a \cos(q_a) \\ c_a \sin(q_a) \end{bmatrix} \quad (18)$$

$$\mathbf{p}_{cd} = \begin{bmatrix} l_a \cos(q_a) + c_d \cos(q_a + q_{ds}) \\ l_a \sin(q_a) + c_d \sin(q_a + q_{ds}) \end{bmatrix}, \quad (19)$$

where $\mathbf{q}_{act}$, l_s, $\mathbf{p}_{ca}$, and $\mathbf{p}_{cd}$ are the actuator angle, spring length, and contact points on link A and link Ds, respectively.

In order to remove the tangential forces/velocities at the contact points, the 2×4 matrix $\mathbf{F}_{norm}$ is defined using the normal vectors at the contacts, $\mathbf{a}_y^T$ and $\mathbf{ds}_y^T$

$$\mathbf{F}_{norm} = \begin{bmatrix} \mathbf{a}_y^T & \mathbf{0}_{1\times 2} \\ \mathbf{0}_{1\times 2} & \mathbf{ds}_y^T \end{bmatrix}. \tag{20}$$

REFERENCES

[1] S. Hirose and Y. Umetani, "The development of soft gripper for the versatile robot hand," *Mechanism and machine theory*, vol. 13, no. 3, pp. 351–359, 1978.

[2] C. Gosselin, "Underactuated mechanical finger with return actuation," *US Patent 5,762,390*, June 1998.

[3] B. Massa, S. Roccella, M. Carrozza, and P. Dario, "Design and development of an underactuated prosthetic hand," in *Proceedings of the 2002 IEEE International Conference on Robotics and Automation*, vol. 4, pp. 3374–3379, 2002.

[4] M. Carrozza, C. Suppo, F. Sebastiani, B. Massa, F. Vecchi, R. Lazzarini, M. Cutkosky, and P. Dario, "The SPRING Hand: Development of a Self-Adaptive Prosthesis for Restoring Natural Grasping," *Autonomous Robots*, vol. 16, pp. 125–141, Mar. 2004.

[5] A. Dollar and R. Howe, "The SDM Hand: A Highly Adaptive Compliant Grasper for Unstructured Environments," in *Experimental Robotics*, pp. 3–11, 2009.

[6] V. Begoc, S. Krut, E. Dombre, C. Durand, and F. Pierrot, "Mechanical design of a new pneumatically driven underactuated hand," in *Proceedings 2007 IEEE International Conference on Robotics and Automation*, pp. 927–933, Apr. 2007.

[7] L. Birglen, T. Laliberté, and C. Gosselin, *Underactuated Robotic Hands*, vol. 40 of *Springer Tracts in Advanced Robotics*. Berlin, Heidelberg: Springer Berlin Heidelberg, 2008.

[8] "Seabed Rig Homepage." `http://seabedrig.no/`, 2011.

[9] L. Demers and C. Gosselin, "Kinematic design of an ejection-free underactuated anthropomorphic finger," in *Proceedings of the 2009 IEEE international conference on Robotics and Automation*, pp. 776–781, 2009.

[10] M. Ciocarlie and P. Allen, "A design and analysis tool for underactuated compliant hands," *Proceedings of the 2009 IEEE/RSJ*, pp. 5234–5239, 2009.

[11] R. Balasubramanian, J. Belter, and A. Dollar, "External disturbances and coupling mechanisms in underactuated hands," in *Proceedings of IDETC/CIE*, 2010.

[12] L. Birglen and C. Gosselin, "Optimal design of 2-phalanx underactuated fingers," in *Proceedings of 2004 International Conference on Intelligent Manipulation and Grasping*, pp. 110–116, 2004.

[13] L. Birglen, "An Introduction to the Analysis of Linkage-driven Compliant Underactuated Fingers," in *Proceedings of IDETC/CIE*, 2006.

[14] G. a. Kragten and J. L. Herder, "The ability of underactuated hands to grasp and hold objects," *Mechanism and Machine Theory*, vol. 45, pp. 408–425, Mar. 2010.

[15] J. McCarthy, *Geometric design of linkages*. New York: Springer, 2000.

[16] S. Montambault and C. M. Gosselin, "Analysis of Underactuated Mechanical Grippers," *Journal of Mechanical Design*, vol. 123, no. 3, p. 367, 2001.

[17] A. Dollar and R. Howe, "The highly adaptive sdm hand: Design and performance evaluation," *The International Journal of Robotics Research*, vol. 29, no. 5, p. 585, 2010.